Comparing the Finite-Difference Schemes in the Simulation of Shunted Josephson Junctions

Valerii Y. Ostrovskii, Artur I. Karimov, Vyacheslav G. Rybin, Ekaterina E. Kopets, Denis N. Butusov
Saint Petersburg Electrotechnical University "LETI"
Saint Petersburg, Russia
{vyostrovskii, aikarimov, vgrybin, eekopets, dnbutusov}@etu.ru

***Abstract*—The paper provides investigation of the numerical effects in finite-difference models of RLC-shunted circuit simulating Josephson junction. We study digital models of the circuit obtained by explicit, implicit and semi-explicit Euler methods. The Dormand-Prince 8 ODE solver is used for verification as a reference method. Two aspects of the RLC-shunted Josephson junction model are considered: the dynamical maps (two-dimensional bifurcation diagrams) and chaotic transients existing in the system within a certain parameter range. We show that both explicit and implicit Euler methods distort the dynamical properties, including stretching or compressing the dynamical maps and changing chaotic transient lifetime decay curve. Experiments demonstrate high reliability of the first-order Euler-Cromer method in simulation of the shunted Josephson junction model which yields data close to the reference data. Obtained results bring new accurate chaotic transient lifetime decay equation for the RLC-shunted Josephson junction model.**

I. Introduction

The systems with Josephson junctions [1] possess the quantum properties of a superconducting state, the effective use of which contributes to the development of many applications, including telecommunications and high-performance computing. The main advantages of superconducting electronics, as an alternative to semiconductor logic circuits, are low power consumption and record-breaking clock rates. The last property allowed to create numerous ultrafast circuits, e.g. rapid single flux quantum digital dividers operating up to 770 GHz [2], digital signal processors clocked at 20 to 40 GHz [3], [4], and serial microprocessors, where operating frequencies approach 20 GHz [5]. Cryocooled prototypes also include router components working at 47 Gbs^{-1} port speed [6] and digital receivers utilized for satellite communications [7].

Since superconductive electronics still comprises a prospective class of elements, only a few general purpose design environments, e.g. SPICE-based simulators, include models of such devices. Circuit simulation is usually performed using circuit representation in a form of ordinary differential or differential-algebraic equations. Some early attempts of simulating inductively shunted Josephson junction were undertaken by Whan and Lobb [8]. Their model, being one of the chaotic Josephson junction based designs, was used as a prototype for some other chaotic generators [9]. Taking into account the progress in numerical analysis of dynamical systems, several details in the original study [8] need some refinement. Particularly, in the numerical experiments authors applied the first order Euler integration method, which could affect the obtained results in chaotic dynamics and bifurcation patterns. This opinion is conditioned by the fact that recent investigation of numerical effects in chaotic systems induced by the application of forward and backward Euler methods [10] reveals notable influence of discrete operators on chaotic behavior. Additionally, among the numerical methods suitable for more reliable chaotic system simulation, semi-explicit and semi-implicit geometrical methods have shown promising results [11], [12].

Therefore, the aim of the current study is to reconsider and probably improve the results of Whan and Lobb [8] for a simple RCL-shunted Josephson junction model using three first-order numerical approaches including the explicit, implicit Euler methods and the semi-explicit Euler-Cromer method. To obtain a reference solution, the high-order explicit Dormand-Prince 8 method was used.

Taking into account recent advances in numerical treatment of chaotic problem, we put forward a hypothesis that application of the semi-explicit method would result in better correspondence to the reference and better reflect dynamical features of the continuous system. We also pursued a goal to manifest the updated experimental data describing chaotic effects occurring in the considered circuit if some new of them will be discovered.

II. RCL-shunted model of Josephson junction

We consider the inductively shunted model of Josephson tunnel junction (RCLSJ) that, being compared with the usual resistively shunted junction model (RSJ), more accurately describes the effects appearing in the circuit with high critical current flow.

A. Circuit equations

The circuit of the RCL-shunted model is shown in Fig. 1. It comprises two parallel branches: the Josephson junction on the left and the shunt on the right.

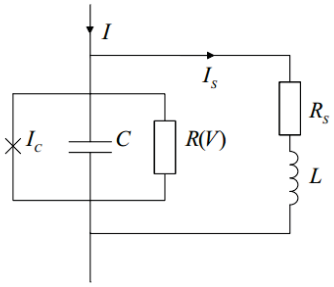

Fig. 1. Schematic sketch of the RCL-shunted Josephson junction circuit

The set of circuit equations for the RCL-shunted model is as follows:

$$\begin{aligned} V &= \frac{\hbar}{2e}\frac{d\gamma}{dt} \\ I &= C\frac{dV}{dt} + \frac{V}{R(V)} + I_C \sin(\gamma) + I_S \\ V &= L\frac{dI_S}{dt} + I_S R_S \end{aligned} \tag{1}$$

where γ is the phase difference of the superconducting order parameter, I_C – critical current, C – capacitance and $R(V)$ – nonlinear resistance of the junction; L is the inductance and R_S is the resistance of the shunt.

B. System equations

Applying the substitutions $x_1 = \gamma \bmod 2\pi$, $x_2 = V / I_C R_S$, $x_3 = I_S / I_C$ and $\tau = 2eI_C R_S t / \hbar$, Eq. (1) can be put into the standard form:

$$\begin{aligned} \frac{dx_1}{d\tau} &= x_2 \\ \frac{dx_2}{d\tau} &= \frac{1}{\beta_C}\left(i - gx_2 - \sin(x_1) - x_3\right) \\ \frac{dx_3}{d\tau} &= \frac{1}{\beta_L}(x_2 - x_3) \end{aligned} \tag{2}$$

where $\beta_C = 2eI_C R_S^2 C / \hbar$ is the Stewart-McCumber parameter, $\beta_L = 2eI_C L / \hbar$ is the dimensionless inductance, $i = I / I_C$ is the external bias current, $g = R_S / R(V)$ is the tunnel junction conductance. The resistance $R(V)$ is set to the value R_N if $|x_2| > V_g / (I_C R_S)$, else $R(V) = R_{sg}$. The parameters of the $Nb/Al_2O_3/Nb$ tunnel junction are $V_g / (I_C R_S) = 6.9$, $R_S / R_N = 0.367$, $R_S / R_{sg} = 0.0478$.

III. Simulation results

We compare three one-step first-order methods of different classes. The first one is the explicit Euler method, known as the simplest but not very reliable and stable method for solving ordinary differential equations. It is also known, that Euler method decreases the parametric stability of the finite-difference scheme in comparison to the continuous prototype [10]. The second one is the implicit Euler method, which possesses *A*-stability, but is known for suppressing chaotic trajectories [10]. The third one is the semi-explicit Euler-Cromer method, widely used for undamped oscillatory problems, but recent experiments proved its superior properties in solving damped chaotic equations [11], [12]. While the theoretical explanations of this superiority remain incomplete, we propose that this would retain for a wide class of chaotic systems, at least conservative ones.

When studying dynamical systems simulations, one needs the reference solution to analyze obtained results. It is extremely hard to obtain analytical solutions of nonlinear ODEs, thus, in our study we used the reference data obtained with the 8th order accurate explicit Dormand-Prince method, which belongs to the family of Runge-Kutta solvers.

The implementation of the semi-explicit Euler-Cromer method applied to the equations (2) is given in Listing 1 in a C-like pseudocode. Notice that the values of `x[0]` and `x[2]` updated on the current integration step are directly used for obtaining `x[1]` within the same step. This special feature distinguishes semi-explicit and semi-implicit methods from explicit and implicit methods. In Listing 1, the constants `p[0]` ÷ `p[5]` are set according to the values of corresponding parameters in the system (2).

Listing 1. Implementation of the Semi-implicit Euler-Cromer method for the dynamical system (2)

```
x[0] = x[0] + h*x[1];
x[2] = x[2] + h*(1/p[0])*(x[1]-x[2]);
x[1] = x[1] + h*((1/p[1])*(p[2]-
       -((x[1]>p[3]) ? p[4] : p[5])*
       *x[1]-sin(x[0])-x[2]));
```

Listings for the forward and backward Euler methods are not given since they are trivial.

A. Overview of the dynamics

The original paper [8] presented a dynamical map of the system (2), which is a two-dimensional generalization of bifurcation diagrams. Such maps are widely used for visual localization of chaotic regions in a multiparametric space. Each pixel of the dynamical map represents a number of periods in the attractor. To verify previously obtained results and to compare three abovementioned numerical methods, we constructed dynamical maps within the same parameter range as in [8]. We also constructed a reference dynamical map with the Dormand-Prince 8 method. All dynamical maps are shown in Fig. 2. In the maps, the pixel tint represents the number of periods, from value of 1 and less (simple periodic or non-periodic behavior) to 20 and more (a chaotic attractor).

The numerical investigation reveals the predicted results. The application of the explicit Euler method leads to the expansion of chaotic regions, as can be seen in Fig. 2 (a). For the implicit Euler method, its property to suppress chaos induced visible decrease of chaotic regions, see Fig. 2 (b). The dynamical map obtained with the semi-explicit Euler-Cromer method closely resembles the dynamical map obtained with the reference method, as it is shown in Fig. 2(c) and Fig. 2(d), respectively. The integration stepsize was set to $h = 0.05$. Its decrease obviously makes the dynamical maps more similar, but one should notice that ability of the method to nearly retain the original properties of the system within the broad range of integration steps allows obtaining maps with a fine resolution for a smaller computational time.

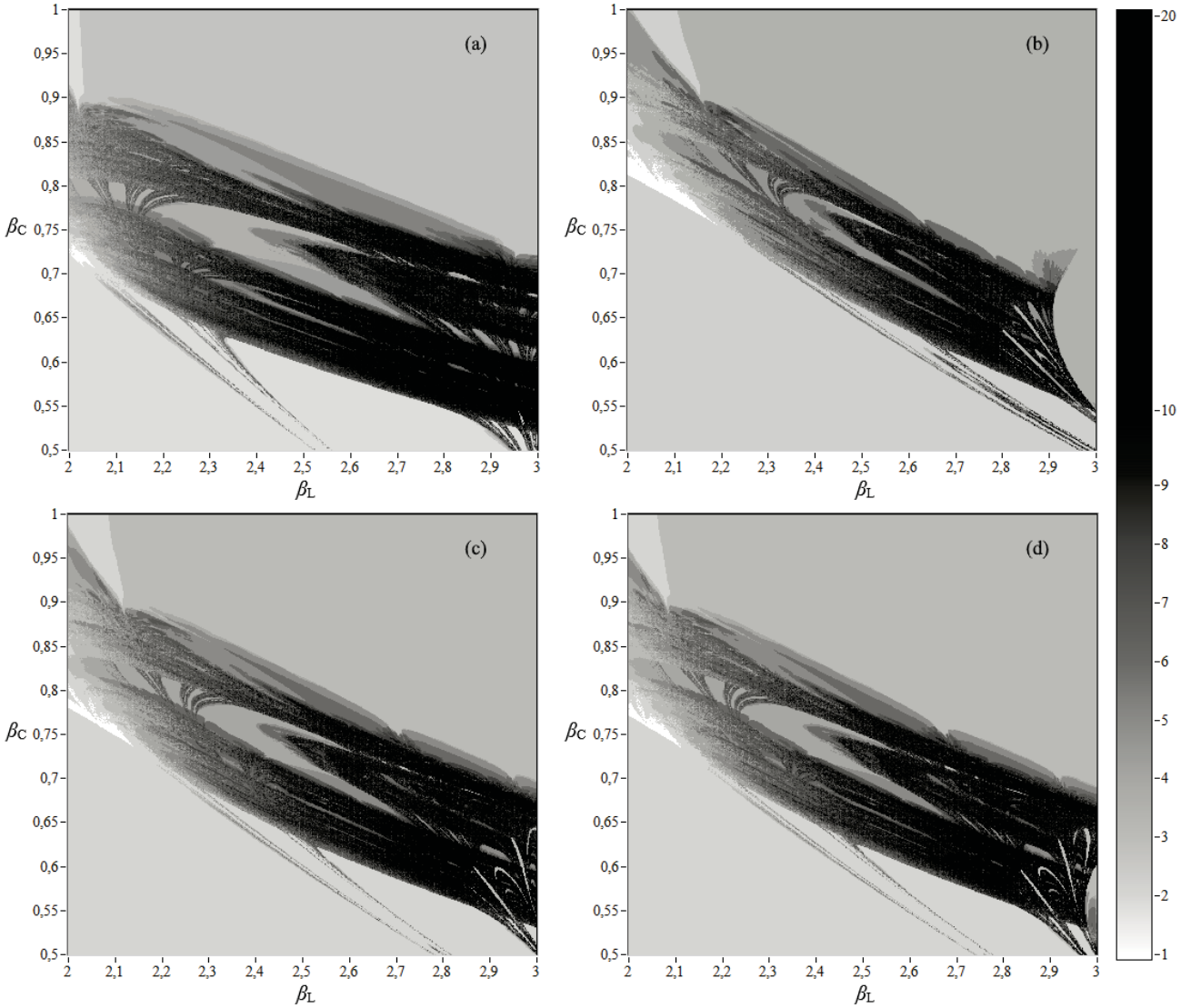

Fig. 2. Dynamical maps of the discrete models of system (2), obtained with (a) explicit Euler, (b) implicit Euler, (c) semi-explicit Euler-Cromer, and (d) explicit Dormand-Prince 8 method. Here the current $i = 1.20$, the stepsize $h = 0.05$.

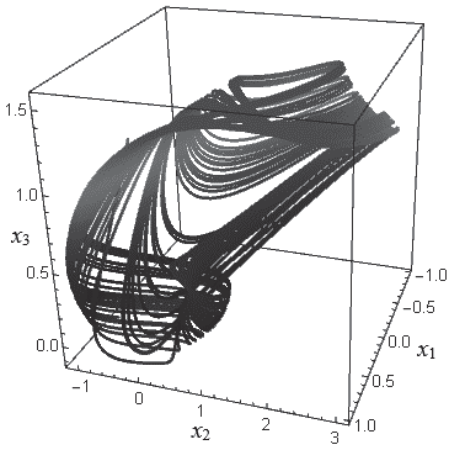

Fig. 3. Chaotic attractor of the system (2), where $\beta_L = 2.6$, $\beta_C = 0.707$, $i = 1.20$

One of the possible shapes of chaotic attractor is given in Fig. 3 for the parameters $\beta_L = 2.6$, $\beta_C = 0.707$, and $i = 1.20$.

B. Chaotic transients

As it was shown by Whan and Lobb [8], dynamics of the system (2) is characterized by chaotic transients preceding the falling into periodic oscillations for an intermediate range of parameter values, for instance, $\beta_L = 29.215$, $\beta_C = 0.707$, $i = 1.25$. However, the paper [8] reports that the chaotic transient is followed by only single type of periodic trajectory, as shown in Fig. 4, top. More accurate numerical investigation reveals another type of periodic trajectory with more complicated dynamics. Thus, in a certain range of parameter values two stable limit cycles coexist in the system (2). A typical transient with the second type limit cycle is shown in Fig. 4 (bottom left) and a periodic process in appropriate time scale is given in Fig. 4 (bottom right).

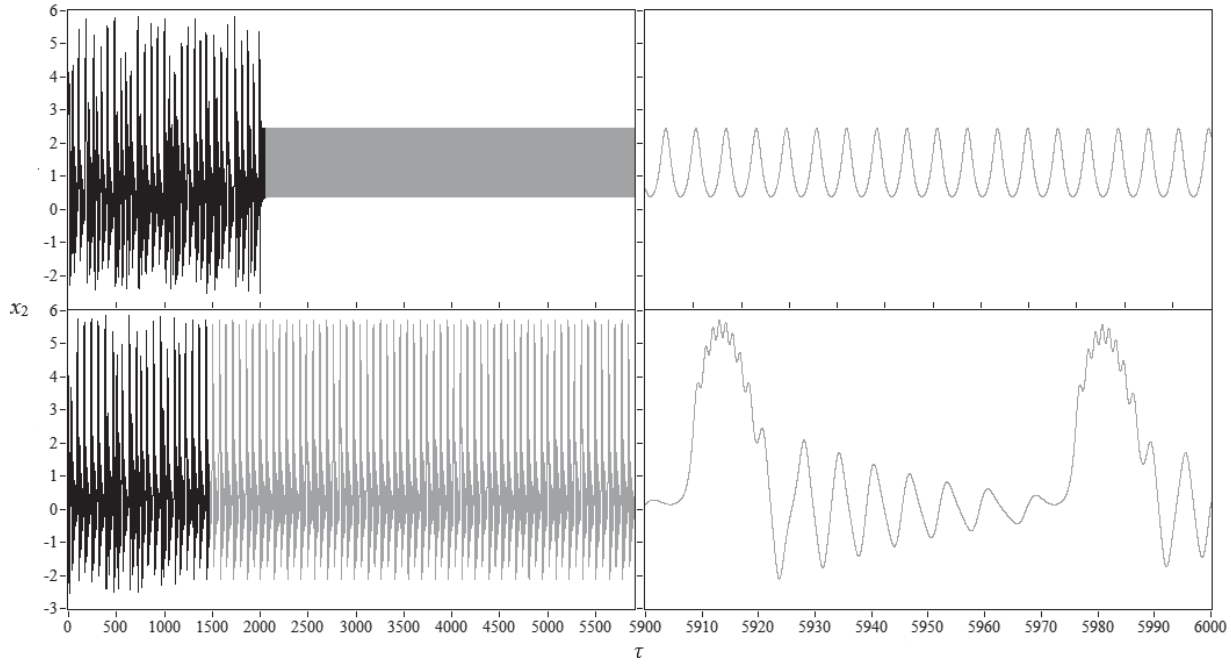

Fig. 4. Chaotic transients (black) and two different periodic attractors (gray) of the system (2). Here $\beta_L = 29.215$, $\beta_C = 0.707$, $i = 1.25$, $h = 0.01$.

The investigation of the lifetimes of chaotic transients shows a strong influence of the integration method on the simulation results. The methodology of the experiment was as follows. From a set of uniformly distributed initial conditions, as it is shown in Fig. 5, trajectories were calculated by four integration methods, namely, explicit Euler, implicit Euler, semi-explicit Euler-Cromer, and explicit Dormand-Prince 8 method. The integration stepsize was similar for each method and was set to $h = 0.01$. For each trajectory we measured a time of chaotic transient. One possible method for detecting the boundary of the chaotic transient is to calculate the largest Lyapunov exponent, and a time interval where it was confidently positive can be considered as a chaotic transient. In practice, this method has strong limitations since the existing largest Lyapunov exponent estimation algorithms have certain latency and do not allow immediate detection of oscillation mode change. A more reliable method is the peak detection, when a set of thresholds is tuned to capture the change in system behavior for both types of periodic solutions. To illustrate this, we plotted lifetimes for 900 trajectories obtained with the implicit Euler method in Fig. 5 (bottom). One can see that the lifetime of the chaotic transient highly depends on initial conditions. A law governing the number of remaining trajectories after a time τ was offered in [13] and can be written as

$$N(\tau) = N(0)e^{-\tau/\langle\tau_{tr}\rangle} \tag{3}$$

where $\langle\tau_{tr}\rangle$ is an average transient lifetime and $N(0)$ is a number of trajectories. The equation (3), describing the exponential decay, is plotted in logarithmic scale as a line with a negative slope. The average lifetime value found in [8] for the first-order Euler method was $\langle\tau_{tr}\rangle = 8293$. Our numerical experiments show that the decay law (3) is asymptotically correct when the explicit and the implicit Euler methods are used. Nevertheless, the values of $\langle\tau_{tr}\rangle$ are sufficiently different and depend on the method, see Fig. 6 (a) and (b). For the explicit Euler method, the average lifetime value was $\langle\tau_{tr}\rangle = 34206.6$, and for the implicit Euler method $\langle\tau_{tr}\rangle = 14940.6$. This discrepancy can be explained by a notable difference in a truncation error behavior of the explicit and implicit methods. Despite the fact that the decay shape meets theoretical predictions (3) well, these results cannot be accounted as reliable.

In our previous papers [11, 12], the semi-explicit Euler-Cromer method and semi-implicit composition methods were shown to be more adequate in chaotic problems simulation. Investigation of the transient time decay in the system (2) simulated with the Euler-Cromer method have shown results that are different from the results obtained with both forward and backward Euler methods. The shape of the decay curve here cannot be described by the rule (3). A nearly horizontal line in the initial interval of the decay curve appeared, indicating almost similar lifetimes for transients with duration 0-300, and the succeeding exponential decay acquired more steep slope than was predicted by the law (3), see Fig. 6 (c). The more accurate decay law, obtained by fitting the experimental curves, comprises a sum of two Gaussian distributions, namely

$$N(\tau) = N_1 e^{-\left(\frac{\tau-\tau_1}{c_1}\right)^2} + N_2 e^{-\left(\frac{\tau-\tau_2}{c_2}\right)^2} \tag{4}$$

where coefficients N_1, N_2, c_1, c_2, τ_1, τ_2 are found numerically. For the semi-explicit Euler-Cromer method, they are $N_1 = 367.1$, $N_2 = 782.9$, $c_1 = 1.57 \cdot 10^4$, $c_2 = 5.51 \cdot 10^4$, $\tau_1 = 7772$, $\tau_2 = -2.82 \cdot 10^4$. The law (4) gives root-mean-square error

(RMSE) 5.51 against RMSE 66.59 given by the law (3) for the experimental data.

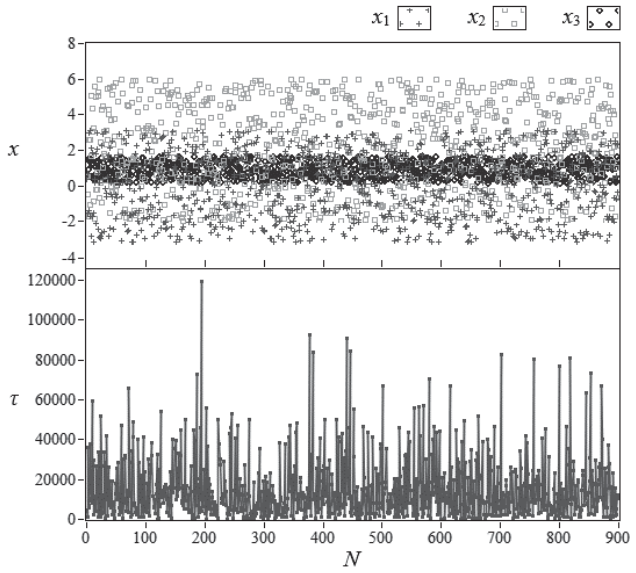

Fig. 5. Random distribution of initial conditions (top) and corresponding lifetimes of chaotic transients obtained with implicit Euler method (bottom)

The decay law (4) persists when a higher order method is applied. The explicit Dormand-Prince method gives almost the same curve, with the average lifetime close to the one obtained with the semi-explicit Euler-Cromer method, which clearly confirms the correctness of the result.

For the high order integrators, the construction of semi-implicit composition methods [14] may appear more accurate for this problem than the Runge-Kutta methods. However, in practice, the law describing the current-voltage characteristics in a real Josephson junction is more complex than one used in our numerical study [15]. Therefore, the practical applicability of the model (1) is restricted by errors in the superconductive devices identification and the accuracy of the first order Euler-Cromer method is enough for the practical purposes.

The results obtained in this section intersect with the data reported in the previous section and prove our prediction that the Euler-Cromer method is the most suitable method for system (2) simulation among the first-order methods.

VII. Conclusion and Discussion

We investigated the numerical effects existing in finite-difference RLC-shunted Josephson junction model obtained by different integration methods. It was clearly shown that the forward and backward Euler methods, often used for numerical studies, lead to notable distortions of the model dynamics. Among the first-order numerical integration methods, the best results from the point of correspondence to the reference data were performed by the Euler-Cromer method. This method belongs to the class of semi-implicit geometrical integrators, which were previously used mostly for Hamiltonian problems. Therefore, our recent results give promising evidence that such type of methods is highly suitable for solving larger class of chaotic problems.

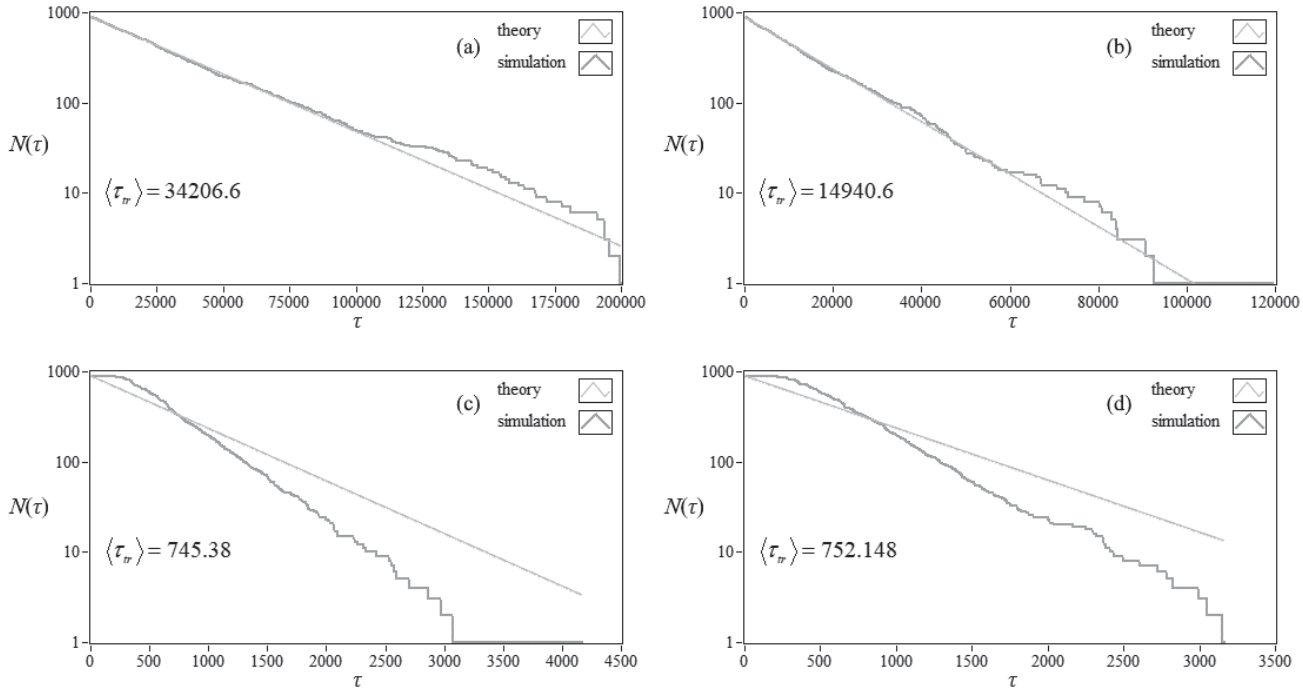

Fig. 6. Decay plots and average lifetimes of chaotic transients, obtained with (a) explicit Euler, (b) implicit Euler, (c) semi-explicit Euler-Cromer, and (d) explicit Dormand-Prince 8 methods. Here $\beta_L = 29.215$, $\beta_C = 0.707$, $i = 1.25$, $h = 0.01$.

Two main aspects of the RLC-shunted Josephson junction model were investigated. First, the dynamical maps, or two-dimensional bifurcation diagrams, were constructed. The distortions clearly induced by explicit and implicit Euler methods were nearly negligible in a case of semi-explicit method. The reason of this superiority lies in phase volume and energy conservation effect, typical for geometric integrators applied to the conservative systems.

The property of phase volume distortion also affects the second aspect of the investigated model dynamics, namely lifetimes of chaotic transients in the Josephson junction. The previously reported sensitive dependence of their lifetimes to initial conditions was described by the statistical exponential law. Our results revealed more complicated distribution, representing a combination of two Gaussian terms instead of a single exponent.

The proper model of the superconductive electronic device based on Josephson effect is required for prospective electronic device design, and as a consequence, for creating modern computer aided design tools. One example of such prospective CAD was NioCAD environment, aimed at development of quantum effects based superconductive electronics [16], unfortunately cancelled later. In our study, we consider only the partial effects of numerical simulation, but some others were out of our consideration. For example, not only truncation error but also round-off error sufficiently affects the chaotic behavior [17]. We did not considered the numerical schemes of higher order in this paper. Nevertheless, taking into account obtained results, we can predict that semi-implicit methods will retain their superiority. From the theoretical point of view, an extensive proof of this fact is required. The key feature of these methods is their influence on phase space geometry, allowing them to conserve the average divergence of the flow in more reasonable limits than explicit or implicit methods for a certain class of dynamical systems. With use of composition rules and reversible stepsize controllers [14], efficient simulation tools can be obtained, allowing to design reliable CAD environments for superconductive electronic devices.

The major unresolved problems briefly outlined here will be the topic of our future investigations. The main directions of the works will be the investigation of high-order composition methods, selection of appropriate fractal composition schemes, experimental study of the other superconductive devices, theoretical refinement of the special features of semi-implicit numerical methods in their application to chaotic problems.

ACKNOWLEDGMENT

The reported study was supported by RFBR, research project No. 17-07-00862.

REFERENCES

[1] B.D. Josephson, “Possible new effects in superconductive tunnelling”, *Physics letters*, vol. 1, no. 7, Jul. 1962, pp. 251-253.

[2] W. Chen et al. “Rapid single flux quantum T-flip flop operating up to 770 GHz”, *IEEE Transactions on Applied Superconductivity*, vol. 9, no. 2, Jun. 1999, pp. 3212-3215.

[3] I.V. Vernik et al., “Cryocooled wideband digital channelizing RF receiver based on low-pass ADC”, *in Extended Abstracts of ISEC’07*, Jun. 2007, pp. 71–74.

[4] A.Y. Herr, “RSFQ baseband digital signal processing”, *IEICE transactions on electronics*, vol. E91-C, no. 3, Mar. 2008, pp. 293-305.

[5] M. Tanaka et al., “Design of a pipelined 8-bit-serial single-flux-quantum microprocessor with multiple ALUs”, *Superconductor Science and Technology*, vol. 19, no. 5, Mar. 2006, S344.

[6] Y. Hashimoto, S. Yorozu, and Y. Kameda, “Development of cryopackaging and I/O technologies for high-speed superconductive digital systems”, *IEICE transactions on electronics*, vol. E91-C, no. 3, Mar. 2008, pp. 325-332.

[7] O.A. Mukhanov et al., “Superconductor digital-RF receiver systems”, *IEICE transactions on electronics*, vol. E91-C, no. 3, Mar. 2008, pp. 306-317.

[8] C.B. Whan and C.J. Lobb, “Complex dynamical behavior in RCL-shunted Josephson tunnel junctions”, *Physical Review E*, vol. 53, no. 1, 1996, 405.

[9] J. Ma, P. Zhou, B. Ahmad, G. Ren, C. Wang, “Chaos and multi-scroll attractors in RCL-shunted junction coupled Jerk circuit connected by memristor”, *PLoS ONE*, vol. 13, no. 1, 2018, e0191120, (doi: 10.1371/journal.pone.0191120).

[10] C. Varsakelis and P. Anagnostidis, “On the susceptibility of numerical methods to computational chaos and superstability”, *Communications in Nonlinear Science and Numerical Simulation,* vol. 33, 2016, pp. 118-132.

[11] D.N. Butusov, V.Y. Ostrovskii, A.I. Karimov and V.S. Andreev, “Semi-implicit composition Methods in memcapacitor circuit simulation”, *International Journal of Embedded and Real-Time Communication Systems (IJERTCS)*, vol.10, Issue 2, Article 3, 2018.

[12] D.N. Butusov, V.Y. Ostrovski and D.O. Pesterev, “Numerical Analysis of Memristor-Based Circuits with Semi-Implicit Methods”, *Proceedings of the 2017 IEEE Russia Section Young Researchers in Electrical and Electronic Engineering Conference (2017 ElConRus)*, Saint Petersburg, Russia, February 1–3, 2017, (doi: 10.1109/EIConRus.2017.7910545).

[13] J.A. Yorke and E.D. Yorke, “Metastable chaos: The transition to sustained chaotic oscillations in a model of Lorenz”, *J. Stat. Phys.*, vol. 21, 1979, pp. 263-277.

[14] D.N. Butusov, S.V. Goryainov, V.S. Andreev, K.I. Barashok and M.N. Kozak, “Fractal Composition ODE solvers based on semi-implicit methods”, *Proceedings of the XXI IEEE International Conference on Soft Computing and Measurements (SCM - 2018)*, Saint Petersburg, Russia, May 23–25, 2018.

[15] O. Vavra et al., “0 and π phase Josephson coupling through an insulating barrier with magnetic impurities”, *Physical Review B*, vol. 74, no. 2, 2006, 020502.

[16] C.J. Fourie and M.H. Volkmann, “Status of superconductor electronic circuit design software”, *IEEE Transactions on Applied Superconductivity*, vol. 23, no. 3, 2013, 1300205-1300205.

[17] E.G. Nepomuceno and E.M. Mendes, “On the analysis of pseudo-orbits of continuous chaotic nonlinear systems simulated using discretization schemes in a digital computer”, *Chaos, Solitons & Fractals*, vol. 95, 2017, pp. 21-32.